Orientational order and vesicle shape

T. Lubensky, Jacques Prost

Classification
Physics Abstracts
61.30 — 62.90 — 82.70D

Orientational order and vesicle shape

T.C. Lubensky ([1,2]) and Jacques Prost([3])

([1]) Department of Physics, University of Pennsylvania, Philadelphia, PA 19104, U.S.A.
([2]) Corporate Research Science Laboratories, Exxon Research and Engineering Co., Annandale, New Jersey 08801, U.S.A.
([3]) Groupe de Physico-Chimie Theorique, ESPCI, 10 Rue Vauquelin, 75231 Paris Cedex 05, France

(Received 16 September 1991, accepted 4 December 1991)

Abstract. — In a membrane with in plane orientational order, the topology determines the total strength of the disclinations and thus controls the total elastic energy. Making use of this remark we discuss the relative stability of spherical vesicles, hollow cylindrical tubules (without caps),disks and tori composed of smectic-C, hexatic or "*n*-atic" membranes.

Under appropriate experimental conditions, amphiphilic molecules in an aqueous environment form bilayer membranes that in turn form closed vesicles, usually with the topology of a sphere. The exact shape of such vesicles, which can be quite complex, depends in general on the pressure difference across their membranes or whether their membranes have spontaneous tendency to bend or not [1]. Membranes can exist in different thermodynamic states with varying degrees of orientational and positional order. At high temperatures, the stable phase is generally the fluid L_α or smectic-A (SmA) phase in which molecular axes are normal to the surface defined by the membrane. At lower temperatures, membranes can condense into a Smectic-C (SmC) phase in which molecules tilt relative to the surface normal or into an hexatic phase in which there is quasi-long-range six-fold bond angle order. Tilted bilayers [2] in what are called the $L_{\beta'}$ phases tend to have both tilt and hexatic order (SmI, SmF, or even SmL). It has not been definitively established whether the $L_{\beta'}$ phases exhibit two-dimensional crystalline order (i.e., have a nonzero shear modulus). There are, however, strong theoretical reasons [3] for believing that two-dimensional membranes fluctuating in three-dimensions cannot exhibit two-dimensional crystalline order, and that the $L_{\beta'}$ phases should be viewed as orientationally ordered phases with large Frank elastic constants. If the membrane of a vesicle with spherical topology were to undergo a freezing transition to a crystalline state, it would necessarily develop disclinations [4], which for large systems cost an enormous amount of energy. Under these conditions, the vesicle might break open and form sheets or cylinders which do not require disclinations.

In this paper, we show that the development of in-plane orientational (SmC, I, F, or hexatic) order can favor a morphology change from a sphere to a cylinder or to a torus provided the membrane Frank elastic moduli are sufficiently large, as they will be if positional correlations arising from incipient crystalline order are well-developed. Our hope is that our calculations will provide a possible basis for understanding a series of experiments on microtubule formation in diacethylene compounds [5], morphological changes in self-assembling phospholipids [6],and ultimately morphological changes occuring in some biological systems [7]. Our calculations are only approximate in that they do not consider the continuum of possible shapes. They also do not include chirality, which certainly is important in the examples cited above [8, 9]. Nevertheless, our calculations show that orientational, rather than crystalline order is sufficient to cause equilibrium shape changes and, in particular, to favor cylindrical or toroidal topologies over spherical ones.

We also show that spherical vesicles with in plane-orientational order must have disclinations whose cores are either orientationally disordered (i.e., in the SmA phase) or are macroscopic pores providing a passage from the interior to the exterior of the vesicle. Thus, we predict that spherical vesicles whose membranes are in an $L_{\beta'}$ phase [10] will have disclinations which might be visible under crossed polarizers, regardless of the degree of crystalline order or the pressure difference across the membrane. If the $L_{\beta'}$ phases had pure hexatic order, there would be 12 disclinations at the vertices of an icosahedron inscribed in the sphere as shown in figure 1. For SmF or SmI order, we expect the 12 disclinations to separate into two groups of six centered at each pole and forming a star defect analogous to that seen in free standing films [11]. We present here only calculations for the pure hexatic case.

In order to keep algebra as simple as possible and still illustrate our point, we will compare the energies of orientationally ordered membranes with the limiting shape of a sphere with or without pores, a cylinder, a flat sheet, and a torus. In reality, however, membrane and vesicle shapes change continuously in response to continuous changes in the degree of orientational order in the membrane [12]. It is thus possible to go continuously from a spherical to a cylindrical shape. In our calculations, this transition will be discontinuous.

To describe SmC and hexatic order, we introduce at each point $\mathbf{x} = (x^1, x^2)$ on the membrane a unit vector $\mathbf{m}(\mathbf{x})$ in the tangent plane of the membrane. For SmC order, $\mathbf{m}(\mathbf{x})$ is truely a vector, invariant under rotations of $2p\pi$ (p is an integer) about the unit surface normal $\mathbf{N}(\mathbf{x})$ erected at $\mathbf{x}$. For hexatics, rotations of $\mathbf{m}(\mathbf{x})$ by $2p\pi/6$ about $\mathbf{N}$ lead to physically equivalent states. More generally, we consider "n-atic order" in which rotations of $\mathbf{m}$ through $2p\pi/n$ produce physically equivalent states. A two-dimensional nematic with an in-plane symmetric-traceless tensor order parameter is an example of a 2-atic. Although, we know of no physical

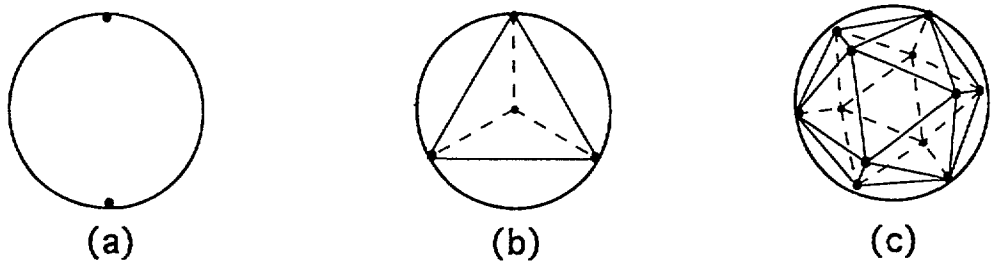

Fig.1. — Equilibrium positions of disclinations for (a) vector ($n = 1$), (b) 2-atic ($n = 2$), and (c) hexatic ($n = 6$) order.

realizations of other n-atics, we find it instructive to consider how the development of such order affects morphological changes in spherical vesicles.

The Frank free energy for an orientationally ordered membrane is a quadratic function of the components of gradients of $\mathbf{m}$ parallel to the surface. For n-atics with $n \geq 3$, there is only one Frank elastic constant. For $n = 1$ or $n = 2$, there are in general two elastic constants. For simplicity. we will consider the single elastic constant approximation from all n:

$$\begin{aligned} F &= \frac{1}{2}K_{\mathrm{A}} \int \mathrm{d}^2x\sqrt{g}[\partial_a \mathbf{m} - \mathbf{N}(\mathbf{N}\cdot(\partial_a \mathbf{m})]^2 \\ &= \frac{1}{2}K_{\mathrm{A}} \int \mathrm{d}^2x\sqrt{g}\mathrm{D}_a m^b \mathrm{D}^a m_b, \end{aligned} \tag{1}$$

where $g = \det g_{ab}$ is the determinant of the metric tensor g_{ab} and $\mathrm{D}_a m^b$ is the covariant derivative of m^b. In this description all n-atics have the same long-wavelength elastic energy. Their properties can differ, however, because their topological excitations, i.e., disclinations are characterized by different strength k. The minimum strength disclination for an n-atic is $1/n$.

The total strength (vorticity) [13] of a vector field on a closed surface with h handles must be $2(1-h)$. Thus, a vector field on the surface of a sphere has total strength 2. The energy of an individual disclination on both flat and curved surfaces is proportional to the square of its strength. It is, therefore, always favorable to form disclinations with the lowest possible strength. In addition, disclinations with the same sign repel each other. These considerations imply that the ground state of a sphere with surface n-atic order will have $2n$ maximally separated disclinations of strength $1/n$. For $n = 1$, there will be two $k = 1$ disclinations at the north and south pole; for $n = 2$, there will be four $k = 1/2$ disclinations at the vertices of a tetrahedron; for $n = 3$, six $k = 1/3$ disclinations at the vertices of an octahedron; and for $n = 6$, twelve $k = 1/6$ disclinations at the vertices of an icosahedron; For $n = 4$, there are eight $k = 1/4$ disclinations that are located at the vertices of a twisted hexahedron obtained by twisting opposite faces of a cube through a relative angle of 45 deg and pushing them slightly together [14]. We have not calculated the equilibrium positions disclinations with other values of n.

The Frank free energy F_n of spherical vesicles with n-atic order and disclinations at the symmetry positions described above can be calculated using a stereographic projection technique[15] described in Appendix I. The result for a shere of radius R is

$$F_n = 2\pi K_{\mathrm{A}}\left[\frac{1}{n}\ln\left(\frac{2R}{r}\right) + f_n\right], \tag{2}$$

where r the radius of the disclination core and f_n is a number that depends only on n (its exact form is given in the appendix). The short distance cutoff r is generally the length scale below which conventional elasticity breaks down. This length diverges as the SmA–SmC transition is approached and becomes of order a molecular length when positional correlations becomes well-developed. The core region can either be disordered (i.e., in the SmA phase) or it can be a pore creating a passage between the interior and the exterior of the vesicle. In the former case, the core energy is proportional to a condensation energy ϵ times the core area πr^2. In the latter case, it is proportional to a line tension γ times the core perimeter $2\pi r$. We consider first the latter case for which the r-dependent part of the energy per disclination becomes

$$K_{\mathrm{A}}\frac{\pi}{n^2}\ln\left(\frac{2R}{r}\right) + 2\pi r\gamma. \tag{3}$$

This energy is minimum for a pore radius

$$r_m = \frac{K_A}{2n^2\gamma} = \frac{\lambda}{2n^2}, \tag{4}$$

where $\lambda = K_A/\gamma$ is the characteristic length determined by Frank elasticity and line tension. When in-plane positional correlations are well-developed, K_A may be significantly larger than typical Frank constants of conventional liquid crystals. More precisely, we expect [16]

$$K_A \simeq K_0(\xi/a_0)^2, \tag{5}$$

where K_0 is the "bare" Frank elastic constant, ξ is the correlation length for positional order, and a_0 is the radius of a molecule in the plane of the membrane. The line tension should not depend strongly on the existence of positional order, and we estimate $K_0/\gamma \simeq a_0$ and

$$\lambda \simeq \frac{\xi^2}{a_0} \text{ or } r_m \simeq \frac{\xi^2}{2n^2 a_0} \tag{6}$$

If positional correlations extend over a large number of molecules, r_m may be very large. For example, it is quite possible for (ξ/a_0) to be of order 100 or larger in hexatics or Smectics-I or F in which crystalline correlations may extend over hundreds of angstroms[17]. In this case, $r_m \approx 10^3$ Å (for Sm-I or Sm-F with $a_0 \approx 5$ A). The existence of such large pores should be experimentally detectable.

The total energy of a vesicle includes the curvature energy F_{cur} that consists of a part arising from mean curvature and from Gaussian curvature[18] (See Appendix II). For a sphere,

$$F_{cur} = 2\pi(4\kappa + \overline{\kappa}), \tag{7}$$

where κ and $\overline{\kappa}$ are, respectively, the mean and Gaussian curvature moduli. The total energy of a sphere with in-plane orientational order and $2n$ disclinations of strength $1/n$ is thus

$$F_s = 2\pi K_A \left[\frac{1}{n}\left(\ln\left(4n^2R/\lambda\right) + 1\right) + f_n\right] + 2\pi(4\kappa + \overline{\kappa}). \tag{8}$$

Note that this energy depends only weakly on the sphere radius. As the system evolves toward a crystalline structure, K_A diverges,. and the energy cost of maintaining a spherical toplogy also diverges. Thus, it is clear that one can expect a morphology change to a state without divergent disclination energies as K_A is increased in a finite size system. This energy decreases with increasing n indicating that it is preferable to create disclinations with the minimum possible strength.

If there are no pores and the cores are disordered, then the free energy of a sphere with n-atic order is identical to equation (8) with $\lambda/(2n^2)$ replaced by $\sqrt{K_A/(2\epsilon n^2)}$. From this, it is easy to see that for large systems, it is always energetically preferable to open up pores. The energy barrier to open such pores may, however, be quite high. In fact closed vesicles with spherical topology and $L_{\beta'}$ membrane order have been reported in the literature[10]. These vesicles should have disclinations.

In what follows, we will consider three limiting geometries: a flat disk, a hollow cylinder without caps, and a torus (Fig. 2). We will compare energy at constant area, $4\pi R^2$, without preserving volume since these structures are all open with the exception of the torus. The latter, however, can be formed from an open structure or be permeable. Depending on boundary conditions, a flat disk may or may not require a disclination. We will consider only the minimum

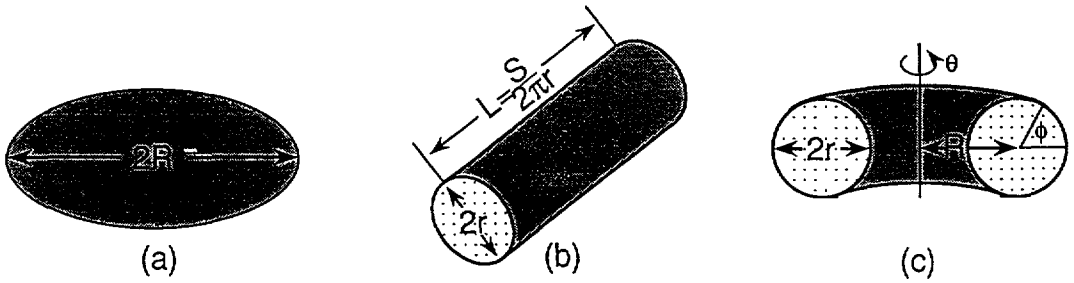

Fig.2. — Schematic representation of (a) disc, (b) an open cylindrical vesicle, and (c) a toroidal vesicle.

energy state without disclinations that results when there are free boundary conditions for bond order at the edges. In this case, a disc only has boundary energy:

$$F_{\rm d} = 2\pi\gamma R_{\rm d} = 4\pi\gamma R, \tag{9}$$

where $R_{\rm d} = 2R$ is the radius of a disc with area $4\pi R^2$. If there were strong anchoring of the orientational order at the edges, there could be a disclination on the disc, but the dominant dependence of $F_{\rm d}$ on R would still be linear (as opposed to logarithmic). Comparisons of equations (9) and (8) shows that discs with radii smaller than $r_{\rm m}/n$ are more stable than spheres. (Note that since these spheres would have pore radii of order the sphere radius, the minimun energy shape is probably some curved disk, which may be the experimentally observed "shards"[19].)

The calculation of the energy of a hollow cylinder is straightforward since it involves only mean curvature and line energy:

$$F_{\rm c} = 4\pi r\gamma + \frac{1}{2}\kappa(\frac{S}{r^2}), \tag{10}$$

where r is the cylinder's radius and S its total area (Fig. 2a). To compare $F_{\rm c}$ and $F_{\rm s}$ with the same number of molecules, we set $S = 4\pi R^2$. Then minimizing $F_{\rm c}$ with respect ot r, we obtain

$$F_{\rm c} = 6\pi\kappa(R/l)^{2/3}, \tag{11}$$

where we have set $l = \kappa/\gamma$. Comparison of (11) and (8) shows that for "very" large systems the sphere with pores is favored over a cylinder. If, however, positional correlations are sufficiently well-developed, $K_{\rm A}$ may be so large that the cylindrical shape is favored. Thus, for example, as $K_{\rm A}$ increases upon cooling, a transition from a sphere to an equal area cylinder could result.

We now consider the torus, which is a structure with one handle and no edges. Since a vector field on its surface will have zero total strength, the state with the lowest Frank free energy F_n will contain no energetically costly disclinations. On the other hand, a torus has a nonzero Gaussian curvature and thus, unlike the cylinder, a nonvanishing value of $F_{\rm curv}$ in the ground state. A large torus is locally very similar to a cylinder, and its Frank free energy for a sufficiently large area will be smaller than the edge energy of a cylinder. Thus, one might expect the torus to be favored at large area. In Appendix II, we show that the ground state of torus constains no disclinations and that its total energy (including both Frank and curvature parts) is

$$F_{\rm t} = 2\pi^2 K_{\rm A}\frac{(1-\sqrt{1-\mu^2})}{\mu} + \frac{2\pi^2\kappa}{\mu\sqrt{1-\mu^2}} \tag{12}$$

where $\mu = r/R$ is the ratio of the principal radii of the torus (Fig. 2c). Note that F_t, unlike F_s, F_d, or F_c does not involve any length scale. For a given μ, one can alway choose R_t so that the area of the torus is πR^2. The lowest energy is thus the minimun of F_t over μ. This leads to the equation

$$s\delta^3 + (2-s)\delta^2 - 1 = 0, \ (0 < \delta < 1) \tag{13}$$

for $\delta = (1-\mu^2)^{1/2}$ where $s = K_A/\kappa$. The solution to this equation for large and small s is

$$\mu_m \simeq \begin{cases} 1/\sqrt{2} & \text{for } s << 1; \\ \sqrt{s/2} & \text{for } s >> 1. \end{cases} \tag{14}$$

The two corresponding limiting behaviors of F_t are

$$F_t \simeq \begin{cases} 4\pi^2\kappa & \text{for } s << 1; \\ 4\pi^2\sqrt{\kappa K_A/2} & \text{for } s >> 1. \end{cases} \tag{15}$$

Because F_t does not depend on size, tori should always be favored for sufficiently large systems. There are probably substantial energy barriers making it kinetically difficult for a sphere to transform to a torus. Tori have, however, been observed recently in phospholipid vesicles[6] and in partially polymerized systems [20] with an aspect ratio $\mu = 1/\sqrt{2}$ appropriate to the case $s = 0$, which should be relevant to this experiment [21 (See Eq. (13)).

In figure 3, we show the stability limits in the (K_A/κ)–(R/l) plane for the various shapes we have considered. We have chosen $\overline{\kappa}/\kappa = 2.20 < 2(\pi - 2)$ so that spheres are favored over tori at small K_A. We have also considered only hexatic order so that the icosahedral arrangement of disclinations occurs on the sphere. At fixed R cylinders are always favored at large s $(= K_A/\kappa)$, i.e., for strong local positional order. Conversely, at fixed s, tori are always the most stable structures at large R.

For example, if we start from a spherical vesicle with a diameter of 20μm in the SmA phase and cool it into a Smectic-I of F phase, it reaches an instability towards a cylinder when $F_s > F_c$ (if we ignore the torus). If we use the reasonable estimate $l \simeq 20$Å, the cylinder is favored when $K_A/\kappa \approx 10^3$ or $\xi/a_0 \approx 10$ if we assume $K_0 \approx \kappa$. This is quite a reasonable figure for Smectic-I or F phases near their transition to the crystalline phase. The cylinder diameter would be $r \simeq (R/l)^{2/3} l \simeq 1$ μm and a length $L \simeq 2r(R/l)^{2/3} \simeq 1000$ μm. These results compare well with experimental observations [5, 19], although, as already stated the experimental systems are more complex than our model since, for example, chirality, which we have ignored, plays an important role in determining their properties.

The rigidity of tubules may be estimated from the energy of a torus. For a given cylinder diameter, the Kuhn length λ_K is determined by $F(\mu = r/\lambda_K) \approx k_B T$. For large K_A, this implies $\lambda_K \sim K_A r/k_B T$. With the numerical estimates used above, one obtains $\lambda_K \sim 10^3 \mu$m, implying that such tubules would be essentially straight. On the other hand, it would be extremely interesting to study experimentally the bending fluctuations of tubules or to measure directly their bending ridigity in a mechanical experiment to obtain a measure of the Frank elastic constant K_A.

Although we have concentrated in this article on the transformation from a sphere to a cylinder and the energy increase associated with pores in the structure, one should keep in mind that spikes may also reduce disclination energy.

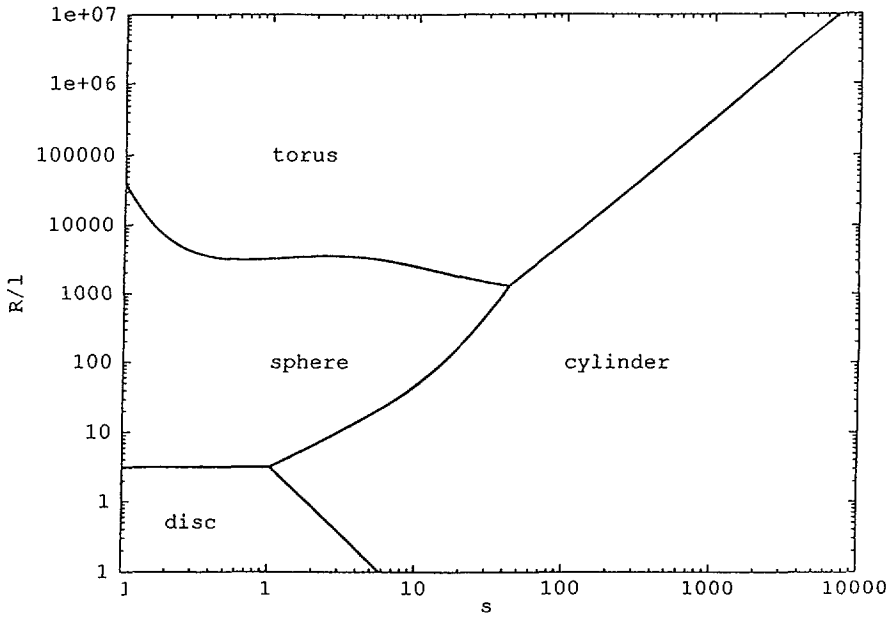

Fig.3. — Phase diagram in the (R/l)-s [$s = K_A/\kappa$] plane, showing regions where disc, spherical, cylindrical, and toroidal vescicles have the lowest free energy. This figure was generated using a Gaussian curvature modulus $\overline{\kappa}$ equal to 2.20κ so that spheres are favored over tori at $K_A = 0$. Hexatic order was also assumed so that the vortices are located at the vertices of an icosahedron inscribed in the sphere.

Acknowledgments.

T.C.L acknowleges partial support for this work from the NSF under grants DMR 88-15469 and DMR 88-19885. We are grateful to Peter Palffy-Muhoray for providing us with numerical verification of the lowest energy configurations of vortices on a sphere and in particular for pointing out to us that the for $n = 4$ vortices are not at the vertices of cube.J.P thanks J.Schnur and the members of the Naval Research Laboratory for very informative conversations.

Appendix I.

In this appendix, we will derive equation (8) for the Frank energy of a sphere with surface n-atic order. We begin by expressing the Frank free energy on a curved surface in terms of the spin connection [3, 22]. In this representation, the unit vector $\mathbf{m}(\mathbf{x})$ with $\mathbf{x} = (x^1, x^2)$ is decomposed into components relative to orthnormal basis vectors $\mathbf{e}_1$ and $\mathbf{e}_2$ in the tangent plane of the surface:

$$\mathbf{m} = \cos\gamma \mathbf{e}_1 + \sin\gamma \mathbf{e}_2, \tag{A1}$$

and

$$F = \frac{1}{2} K_A \int \mathrm{d}^2x \sqrt{g} g^{ab} (\partial_a \gamma - A_a)(\partial_b \gamma - A_b) \tag{A2}$$

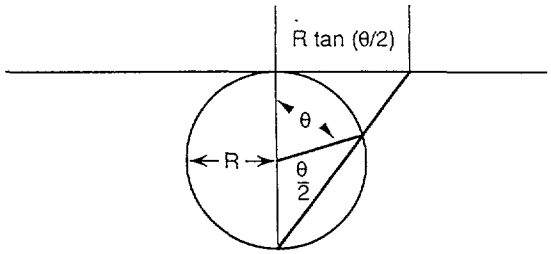

Fig.4. — The sterographic mapping of the sphere onto the complex plane. We have chosen to place the sphere below the projection plane so that a positive disclination on the projection plane corresponds to a positive disclination on the sphere.

where $A_a = \mathbf{e}_1 \cdot \partial_a \mathbf{e}_2$ and $g^{ab} = (g^{-1})_{ab}$. We can choose $\mathbf{e}_1 = \mathbf{e}_\theta$ and $\mathbf{e}_2 = \mathbf{e}_\phi$ to be the standard basis on a sphere. For reasons which will become clear, we will use a stereographic projection gauge [15] to carry out our calculations. In this gauge, each point $\mathbf{R}(\theta, \phi)$ on a sphere is represented as a coordinate $z = 2R\tan(\theta/2)e^{i\phi}$ in the infinite complex plane as depicted in figure 4. The two independent coordinates in the complex plane are chosen to be $x^1 = z$ and $x^2 = \overline{z}$, we obtain

$$g_{ab} = \frac{\partial \mathbf{R}}{\partial x^a} \cdot \frac{\partial \mathbf{R}}{\partial x^b} = \frac{1}{2[1 + (z\overline{z}/4R^2)]^2} \begin{pmatrix} 0 & 1 \\ 1 & 0 \end{pmatrix} \tag{A3}$$

and

$$A_1 = A_z = \mathbf{e}_\theta \cdot \partial_z \mathbf{e}_\phi = -\frac{1}{2iz} \frac{1 - (z\overline{z}/4R^2)}{1 + (z\overline{z}/4R^2)} = \overline{A}_2 = \overline{A}_{\overline{z}} \tag{A4}$$

The Frank free energy is then

$$F = K_A \int \mathrm{d}^2 z \left| \frac{\partial \gamma}{\partial z} - A_z \right|^2, \tag{A5}$$

where $\mathrm{d}^2 z = \mathrm{d}z\mathrm{d}\overline{z}/2$. When $\gamma = 0$, there is a $+1$ disclination at both the north and south poles described by the $\mp 1/(2iz)$ behavior of A_z as $z \to 0$ or ∞. In this case, the Frank free energy is simply

$$F_1 = 2\pi K_A \left[\ln\left(\frac{2R}{r}\right) - 1 \right], \tag{A6}$$

where as before R is the radius of the sphere and r is the radius of a disclination core.

Because the divergence of A_z is zero ($\partial_z A_{\overline{z}} + \partial_{\overline{z}} A_z = 0$), the Euler-Lagrange equation for γ is simply Laplace's equation:

$$\partial_z \partial_{\overline{z}} \gamma = 0. \tag{A7}$$

The solution,

$$\gamma = q_i \mathrm{Im} \ln(z - z_i), \tag{A8}$$

to equation (A7) has a disclination in γ of strength q_i at the inverse image of z_i on the sphere. It also has a disclination of strength $-\infty$. This is easily seen from $\gamma \sim q_i \phi$ as $|z| \to \infty$. Thus, γ increases with clockwise rotation about the unit normal $-\mathbf{e}_z$ at the south pole, and there is a disclination of strength $-q_i$. In general, the solution,

$$\gamma = \sum_i q_i \mathrm{Im}(z - z_i) = \sum_i q_i \gamma_i, \tag{A9}$$

has disclinations of strength q_i at z_i and one of strength $-Q = -\sum_i q_i$ at the south pole. The total strength in the vector $\mathbf{m}$ at the north and south pole include the contributions from the basis vectors $\mathbf{e}_1$ and $\mathbf{e}_2$ and are, respectively, $1+q_0$ and $1-Q$ where q_0 is the strength of γ at $z=0$.

Using equations (A5) and (A9), we can calculate F using standard procedures. We must, however, fix the core radius on the sphere. The image of a circle of radius $r << R$ on the reference sphere whose projection image is centered at z_i is a circle of radius $r_i = (1+|z_i|^2/4R^2)r$. In addition, since the core region from the disclination at the south pole corresponds to the region $|z| > 4R^2/r$ in the projection plane, integrals over d^2z are restricted to $|z| < 4R^2/r$. With this result,

$$F = S + L + F_1 \tag{A10}$$

where S is the contribution to F from the $|\partial_z\gamma|^2$ term and L that from the $\partial_z\gamma - A_z$ cross term. Using

$$\int \mathrm{d}^2z|\partial_z\gamma_i|^2 = \frac{\pi}{2}\ln\frac{4R^2}{rr_i} \tag{A11}$$

and

$$\int \mathrm{d}^2z\partial_z\gamma_i\partial_{\bar{z}}\gamma_j = \frac{\pi}{2}\ln\frac{4R^2}{r|z_i-z_j|}, \tag{A12}$$

we find

$$S = -\pi K_A{\sum_{i\neq j}}' q_iq_j\ln\frac{d_{ij}}{r} + 2\pi K_AQ{\sum_i}' q_i\ln\frac{d_{i\infty}}{r} \tag{A13}$$

where the prime on the sum indicates all disclinations except those at the poles. The distance

$$d_{ij} = \frac{|z_i-z_j|}{\sqrt{1+|z_i|^2/4r^2}\sqrt{1+|z_j|^2/4r^2}} \tag{A14}$$

is the length of the cord separating the inverse images of z_i and z_j, and $d_{i\infty}$ is the length of the cord connecting the inverse image of z_i and the south pole. This result reduces to that of Ovrut and Thomas[11] when $Q=0$. Note that S can be written more compactly as $-\pi K_A\sum_{i\neq j} q_iq_j\ln(d_{ij}/r)$ where the sum is now over all disclinations including that of strength $-Q$ at the south pole. The cross term is

$$L = -2\pi K_A{\sum_i}' q_i[\ln(d_{i0}/r) + \ln(d_{i\infty}/r)] + 2\pi K_AQ\ln(d_{0\infty}/r) \tag{A15}$$

where d_{i0} is the length of the chord connecting the inverse image of z_i to the north pole and $d_{0\infty} = 2R$. Note that L describes the repulsive interaction between the disclinations in γ and the two described by the coordinate system. Combining Equations (A13), (A15) and (A6), we find

$$F_n = -\pi K_A\sum_{i\neq j=1}^{2n} q_iq_j\ln(d_{ij}/r) + 2\pi K_A[2\ln(2R/r) - 1], \tag{A16}$$

where the sum is over all disclinations including those with strength $1+q_0$ and $1-Q$ at the north and south poles. The total vorticity is $1+q_0+(\sum_i' q_i - q_0)+1-Q = 2$ as required. The cord d_{ij} is equal to $2R\sin(\Theta_{ij}/2)$ where Θ_{ij} is the angle between the position vectors relative to the origin of the sphere of vortices i and j. Therefore, the minimum of F_n has the form of equation (2) with

$$f_n = [-\frac{1}{2n^2}\sum_{i\neq j}\ln\sin(\Theta_{ij}/2) - 1]_{\min(\theta_i,\phi_i)} \tag{A17}$$

For $n = 1, 2, 3$, and 6 the vortices in the minimum energy configuration[14] are respectively at the two poles and at the vertices of a tetrahedron, an octahedron, and an icosahderon with

$$\begin{aligned} f_1 &= -1 \\ f_2 &= \frac{3}{4}\ln\left(\frac{3}{2}\right) - 1 \\ f_3 &= \frac{2}{3}\ln(2) - 1 \\ f_6 &= \frac{5}{6}\ln\left(\frac{1+\tau^2}{\tau}\right) - 1 \end{aligned} \tag{A18}$$

where $\tau = (\sqrt{5}-1)/2$ is the golden mean. This result is summarized in equation (9) in the text. When $n = 4$, vortices are not at the vertices of a cube in the equilibrium configuration. Rather the repulsive interaction between vortices is minimized by rotating two opposite faces of a cube through 45 deg and reducing slightly their distance.

Appendix II.

In this appendix we will calculate the Frank and bending energies for a torus. Any point **R** on a torus can be parameterized by the angles $x^1 = \theta$ and $x^2 = \phi$ shown in figure 2c:

$$\mathbf{R}(\theta, \phi) = R\mathbf{e}_\rho + r\mathbf{e}_\phi, \tag{B1}$$

where $\mathbf{e}_\rho = \cos\theta\mathbf{e}_x + \sin\theta\mathbf{e}_y$ and $\mathbf{e}_\phi = \cos\phi\mathbf{e}_\rho + \sin\phi\mathbf{e}_z$ where $\mathbf{e}_x$, $\mathbf{e}_y$, and $\mathbf{e}_z$ are the usual cartesian basis vectors. The metric tensor is then

$$g_{ab} = \begin{pmatrix} (R + r\cos\phi)^2 & 0 \\ 0 & r^2 \end{pmatrix} \tag{B2}$$

and its inverse is

$$g^{ab} = \begin{pmatrix} (R + r\cos\phi)^{-2} & 0 \\ 0 & r^{-2} \end{pmatrix}. \tag{B3}$$

If we choose $\mathbf{e}_1 = -\sin\theta\mathbf{e}_x + \cos\theta\mathbf{e}_y$ and $\mathbf{e}_2 = -\sin\phi\mathbf{e}_\rho + \cos\phi\mathbf{e}_z$, then the components of the connection are

$$A_\theta = -\sin\phi, \qquad A_\phi = 0. \tag{B4}$$

Thus, the Frank energy is

$$F = \frac{1}{2}K_A \int_0^{2\pi} d\theta \int_0^{2\pi} d\phi\, r(R + r\cos\phi)\left[(R + r\cos\phi)^{-2}(\partial_\theta\gamma - \sin\phi)^2 + r^{-2}(\partial_\phi\gamma)^2\right] \tag{B5}$$

The Euler-Lagrange equation for γ is

$$r(R + r\cos\phi)^{-1}\partial_\theta^2\gamma + r^{-1}(R + r\cos\phi)\partial_\phi^2\gamma - \sin\phi\partial_\phi\gamma = 0. \tag{B6}$$

A simple solution to this equation is

$$\gamma = k(\theta - \theta_0) + \gamma_0, \tag{B7}$$

where k is an integer. The associated Frank energy is

$$F = 2\pi^2 K_A \frac{\mu}{\sqrt{1-\mu^2}}\left[k^2 + \frac{\sqrt{1-\mu^2}(1-\sqrt{1-\mu^2})}{\mu^2}\right] \tag{B8}$$

where $\mu = r/R$. This energy is clearly a minimum when $k = 0$, i.e., when $\mathbf{m} = \cos\gamma_0 \mathbf{e}_1 + \sin\gamma_0 \mathbf{e}_2$ rotates with the local reference frame.

The calculation of the curvature energy is a textbook exercise in differential geometry. The curvature tensor is

$$K_{ab} = \mathbf{e}_\phi \cdot \partial_a \partial_b (R\mathbf{e}_\rho + r\mathbf{e}_\phi) = \begin{pmatrix} -\cos\phi(R + r\cos\phi) & 0 \\ 0 & -r \end{pmatrix} \tag{B9}$$

Then using equation (B3) for the contravariant metric tensor, we find

$$K_a^b = \begin{pmatrix} -\cos\phi(R + r\cos\phi)^{-1} & 0 \\ 0 & -r^{-1} \end{pmatrix} \tag{B10}$$

Thus the mean and Gaussian curvatures are, respectively,

$$K_a^a = -\left[\frac{\cos\phi}{(R + r\cos\phi)} + \frac{1}{r}\right] \tag{B11}$$

and

$$G = \det K_a^b = \frac{\cos\phi}{r(R + r\cos\phi)}. \tag{B12}$$

The mean and Gaussian curvature energies are, respectively,

$$F_{\text{mean}} = \frac{1}{2}\kappa \int \mathrm{d}\theta \mathrm{d}\phi \sqrt{g} (K_a^a)^2 = \frac{2\pi^2 \kappa}{\mu\sqrt{1 - \mu^2}} \tag{B13}$$

$$F_{\text{Gauss}} = \frac{1}{2}\bar{\kappa} \int \mathrm{d}\theta \mathrm{d}\phi \sqrt{g} G = 0. \tag{B14}$$

Equations (B8) and (B13) yield equation (13) in the text.

References

[1] Deuling H.J., Helfrich W., *J. Phys. France* **37** (1976) 1335;
Svetina S. and Zeks B., *Biomed. Biochem. Acta.* **43** (1983) 86;
Sackmann E., Duwe H.-P. and Engelhardt H., *Faraday Discuss. Chem. Soc.* **81** (1986) 281.

[2] Smith G.S., Sirota E.B., Safinya C.R., Plano R.J. and Clark N.A., *J. Chem. Phys.* **92** (1990) 4519.

[3] Nelson D.R. and Peliti L., *J. Phys. France* **48** (1987) 1085.

[4] de Gennes P.G., *C.R. Acad. Sci France* **304** (1987) 259.

[5] Geoger J.H., Singh A., Price R.R., Schnur J.M., Yager P. and Schoen P.E., *J. Am. Chem. Soc.* **109** (1987) 6169.

[6] Rudolph A.S., Ratna B.R. and Kahn B., to be published in *Nature*.

[7] Alberts B., Bray D., Lewis J., Raff M., Roberts K. and Watson J.D., Molecular Biology of the Cell, (Garland Publishing, N.Y., 1989) Chap. 10. In fact the problems raised by biological microtubules are more complex because these systems are usually not in thermodynamic equilibirum.

[8] Helfrich W. and Prost J., *Phys. Rev. A* **38** (1988) 3065.

[9] Zhong-can Ou-Yang and Ji-xing Liu, *Phys. Rev. Lett.* **65** (1990) 1679.

[10] Needham D. and Evans E., *J. Phys. Chem.* **91** (1987) 4219.

[11] Dierker S.B., Pindak R. and Meyer R.B., *Phys. Rev. Lett.* **56** (1986) 1819.

[12] Lubensky T.C. and MacIntosh F. (preprint).

[13] See for example, Spivak, M. A Comprehensive Introduction to Differential Geometry (Publish or Perish, Berkeley, 1979); in Liquid Crystals the connection between disclination strength and topology has been exploited first in nematics: Nabarro F., Fundamental aspects of dislocation theory, NBS Spec. Publ. 317 (1970).

[14] Palffy-Muhoray P., private communication.

[15] Ovrut B. A. and Thomas S., *Phys. Rev. D* **43** (1991) 1314.

[16] Nelson D.R. and Halperin B.I., *Phys. Rev.* **19** (1979) 2457.

[17] Pindak R., Moncton D.E., Davey S.C. and Goodby J.W., *Phys. Rev. Lett.* **46** (1981) 1135.

[18] Helfrich W., Z. Naturforsch **28a** (1973) 693; *J. Phys. France* **47** (1986) 321.

[19] Yager P., Schoen P.E., Davis C., Rice R.R. and Singh A., *Chem. Phys. Lipids* **48** (1988) 215.

[20] Mutz M. and Bensimon D. (preprint).

[21] The experimentally observed $\mu = 1/\sqrt{2}$ requires the existence of spontaneous curvature if the minimization is to be performed at constant volume and area (see [20, 9]).

[22] The spin connection is related to the Gaussian curvature by $\sqrt{g}\det K = \epsilon^{ab} D_a A_b$ where ϵ^{ab} is the anti-symmetric tensor.